

# Ground States of the Mean-Field Spin Glass with 3-Spin Couplings

Stefan Boettcher and Ginger E. Lau

<sup>1</sup>*Department of Physics, Emory University, Atlanta, GA 30322, USA*

We use heuristic optimization methods in extensive computations to determine with low systematic error ground state configurations of the mean-field  $p$ -spin glass model with  $p = 3$ . Here, all possible triplets in a system of  $N$  Ising spins are connected with a bond. This model has been of recent interest, since it exhibits the “overlap gap condition”, which should make it prohibitive to find ground states asymptotically with local search methods when compared, for instance, with the  $p = 2$  case better-known as the Sherrington-Kirkpatrick model (SK). Indeed, it proves more costly to find good approximations for  $p = 3$  than for SK, even for our heuristic. Compared to SK, the ground-state behavior for  $p = 3$  is quite distinct also in other ways. For SK, finite-size corrections for large system sizes  $N \rightarrow \infty$  of both, the ensemble average over ground state energy densities and the width of their distribution, vary anomalously with non-integer exponents. In the  $p = 3$  case here, the energy density and its distribution appear to scale with  $\ln N/N$  and  $1/N$  corrections, respectively. The distribution itself is consistent with a Gumbel form. Even more stark is the contrast for the bond-diluted case, where SK has shown previously a notable variation of the anomalous corrections exponent with the bond density, while for  $p = 3$  no such variation is found here. Hence, for the 3-spin model, all measured corrections scale the same as for the random energy model (REM), corresponding to  $p = \infty$ . This would suggest that all  $p$ -spin models with  $p \geq 3$  exhibit the same ground-state corrections as in REM.

## I. INTRODUCTION

Although conceived as a model to represent the properties of disordered magnetic materials [1], Ising spin glasses – and in particular, their mean-field versions such as the Sherrington-Kirkpatrick model (SK) [2] – have found manifold applications in various areas of science and engineering [3]. One especially vibrant area of research has been the study of heuristics to solve NP-hard combinatorial problems, for which such a spin glass with its Boolean degrees of freedom provides about the most concise formulation of a complex, hard-to-solve model [4]. As such, it is essentially equivalent to the quadratic unconstrained binary optimization problem (QUBO) [5] more commonly used in computer sciences and operations research (although some care must be taken with the QUBO formulation [6]). For instance, QUBO has become a benchmark problem for the application of quantum computing to potentially solve NP-hard problems efficiently, at least, since the emergence of the D-Wave quantum computer [7–9], which launched a slew of “quantum-inspired” solvers typically relying on vastly improved parallel processing hardware, such as Simulated Bifurcation [10, 11], Digital Annealer [12], etc.

It is mostly for theoretical reasons that generalizations have been introduced extending SK towards higher-order interactions beyond the basic Ising spin glass, in which two-body interactions are represented by bonds that constrain the behavior of two mutually connected spins. For example, our study here was initially motivated by recent results on the “overlap gap” property [13], which makes finding global minima with local search prohibitive, that was shown to apply to the 3-spin model but not SK [14]. The  $p$ -spin model features  $p$ -body terms coupling together all possible combinations of  $p$  spins with a collective bond. For any positive integer  $p$  and system size

$N$ , their Hamiltonian is given by

$$H(\vec{\sigma}) = - \sum_{1 \leq i_1 < i_2 < \dots < i_p \leq N} J_{i_1 i_2 \dots i_p} \sigma_{i_1} \sigma_{i_2} \dots \sigma_{i_p}, \quad (1)$$

where  $\sigma_i = \pm 1$  are classical Ising spin variables and the bonds  $J$  are drawn randomly from some distribution  $\mathcal{P}(J)$  of zero mean and unit variance. Most notable, it provides a means to interpolate between SK (which corresponds to  $p = 2$ ) and probably the most simple non-trivial spin glass called the random energy model (REM), attained for  $p \rightarrow \infty$  [15, 16]. The  $p$ -spin model also resembles the iconic  $K$ -SAT problem in computer science [17], correspondingly connecting  $K$  Boolean variables in each logical clause.

Our numerical results here support a sharp distinction between SK ( $p = 2$ ) and  $p \geq 3$  in their ground state behavior. Focusing on ground state energies of  $H$  in Eq. (1) and their distribution over the ensemble with bimodal bonds  $J/J_0 = \pm 1$  in units of

$$J_0 = \sqrt{\frac{2}{N^{p-1} p!}}, \quad (2)$$

we find results that resemble those of REM, which would imply that there is also a commonality for all  $p \geq 3$  in the low-temperature limit. This finding is buttressed by studies of a bond-diluted version of the  $p = 3$  model, which exhibits virtually indistinguishable results asymptotically, unlike for SK, where finite size corrections were found to depend strongly on the dilution [18, 19]. The dramatic change in ground state behavior between  $p = 2$  and  $p = 3$  is all the more remarkable as it resembles a similar distinction in the thermodynamic properties between SK, which has a finite-temperature phase transition of 2nd order, and the family of  $p$ -spin models for all  $p \geq 3$  having a finite-temperature phase transition that

N	Complete ( $q = 1$ )			Diluted ( $q = 0.25$ )	
	$n_I$	$\langle e_0 \rangle_N$	$\sigma(e_0)$	$n_I$	$\langle e_0 \rangle_N / \sqrt{q}$
16	100000	-0.6751(1)	0.03030(9)	10000	-0.6695(5)
18	100000	-0.6870(1)	0.02807(8)	10000	-0.6826(5)
20	100000	-0.6977(1)	0.02565(8)	10000	-0.6935(4)
22	100000	-0.7059(1)	0.02396(7)	10000	-0.7026(4)
24	100000	-0.7135(1)	0.02227(7)	10000	-0.7107(4)
26	100000	-0.7197(1)	0.02095(6)	10000	-0.7181(3)
28	100000	-0.72531(9)	0.01966(6)	10000	-0.7241(3)
30	100000	-0.73001(9)	0.01857(6)	10000	-0.7288(3)
32	100000	-0.73436(8)	0.01751(5)	10000	-0.7331(2)
34	100000	-0.73816(8)	0.01670(5)		
36	100000	-0.74167(7)	0.01585(5)	100000	-0.74063(8)
38	100000	-0.74461(7)	0.01508(5)		
40	100000	-0.74754(7)	0.01438(4)		
42	100000	-0.75008(7)	0.01381(4)		
44	100000	-0.75250(6)	0.01318(4)	100000	-0.75172(6)
46	100000	-0.75462(6)	0.01270(4)		
48	100000	-0.75673(5)	0.01218(4)		
50	100000	-0.75854(5)	0.01174(3)		
52	100000	-0.76047(5)	0.01138(4)	56000	-0.75996(8)
54	100000	-0.76197(5)	0.01096(3)		
56	100000	-0.76362(5)	0.01063(3)		
58	80000	-0.76484(6)	0.01019(4)		
60	66000	-0.76635(6)	0.00997(4)	22000	-0.7661(1)
64	30000	-0.76883(8)	0.00937(5)	16000	-0.7686(1)
70	10000	-0.7721(1)	0.00855(9)	10000	-0.7717(1)
80	10000	-0.7765(1)	0.00764(8)	10000	-0.7764(1)
98	10000	-0.7823(1)	0.00621(6)	10000	-0.7822(1)
128	8000	-0.7887(1)	0.00480(5)	3000	-0.7882(1)
160	5000	-0.7928(1)	0.00377(5)	2000	-0.7928(1)
194	2800	-0.7959(1)	0.00313(6)		
256	500	-0.7997(1)	0.0023(1)	200	-0.7996(2)

Table I. List of all data obtained for the 3-spin model for average ground state energies  $\langle e_0 \rangle_N$  and its deviation  $\sigma(e_0)$ . For each system size  $N$ , these observables were averaged over  $n_I$  instances, drawn at random from the ensemble, using the approximate optima reached with the EO heuristic. Columns on the left pertain to the complete (undiluted) system, while those further on the right concern systems that are diluted such that only 25% of the bonds are non-zero (bond density  $q = 0.25$ ).

is of random first order [20]. The similarity of our results for  $p = 3$  and those of REM ( $p = \infty$ ) suggest a relatively small distinction between models for all  $p \geq 3$ , all essentially behaving REM-like at  $T = 0$ .

In Tab. I we have listed all our data for the ensemble average of the ground state energies for both, the complete and the diluted 3-spin system, as well as the deviation in the distribution of ground state energies for the complete system. To analyze the data for its asymptotic

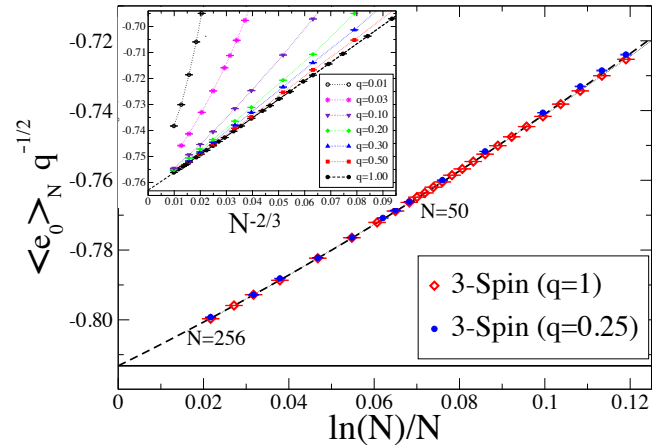


Figure 1. Extrapolation plot for the average ground state energy densities  $\langle e_0 \rangle_N$  as a function of system size  $N$ . Shown is the data for the 3-spin model for the completely connected case, i.e., having bond density  $q = 1$  (red  $\diamond$ ), and for a bond density of  $q = 0.25$  (blue  $\bullet$ ). The most consistent form of finite size corrections, such that the data extrapolates at the  $y$ -intercept to the known thermodynamic limit at  $N \rightarrow \infty$  of  $\langle e_0 \rangle_{N=\infty} = -0.8132$  (indicated by the horizontal line), proves to be  $C_N = \ln N/N$ , with the dashed line providing a quadratic fit in this variable for fixed  $\langle e_0 \rangle_{N=\infty}$ . Inset: Corresponding data for SK up to  $N = 1024$  for varying bond densities  $q$ , from Ref. [18], on a scale of  $C_N = N^{-\frac{2}{3}}$ . Note the much more significant variation in corrections with  $q$  in SK compared to the 3-spin model.

properties, we have first arranged the energies  $\langle e_0 \rangle_N$  in an extrapolation plot according to some presumed form of the finite-size corrections (FSC),

$$\langle e_0 \rangle_N \sim \langle e_0 \rangle_\infty + AC_N + \dots, \quad (N \rightarrow \infty), \quad (3)$$

where  $C_N$  is the expected correction that should vanish for  $N \rightarrow \infty$ . In SK, it is generally believed that  $C_N$  has a power-law form,  $C_N \sim N^{-\omega}$ , and several studies have conjectured that  $\omega = \frac{2}{3}$  for the corrections exponent [21–23], for which the SK ground state data, when plotted according to the FSC in Eq. (3), provides an excellent extrapolation to the exactly-known Parisi energy,  $\langle e_0 \rangle_\infty^{\text{SK}} = -0.76321\dots$  in the thermodynamic limit (see inset of Fig. 1). For the 3-spin model here, such a power-law fit to the data in Tab. I also allows for an exceptionally close fit for all  $N \geq 20$ , with a fitted exponent that is within 1% of  $\omega = \frac{4}{5}$ . However, the extrapolation predicts a fitted value of  $-0.8151(1)\dots$  for the ground state energy density at  $N = \infty$ , which is unacceptable, since it is some  $20\sigma$  from the exactly-known value of  $\langle e_0 \rangle_\infty^{p=3} = -0.8132\dots$ , based on 1-step replica calculations [24, 25]. Fixing  $\langle e_0 \rangle_\infty^{p=3}$  in the power-law fit does not produce a stable result anymore, even when higher-order corrections are included. While it is, of course, impossible to exclude more exotic forms for  $C_N$ , or the effect of higher-order terms, the proximity of a power-law exponent quite close to unity suggests a correction of the

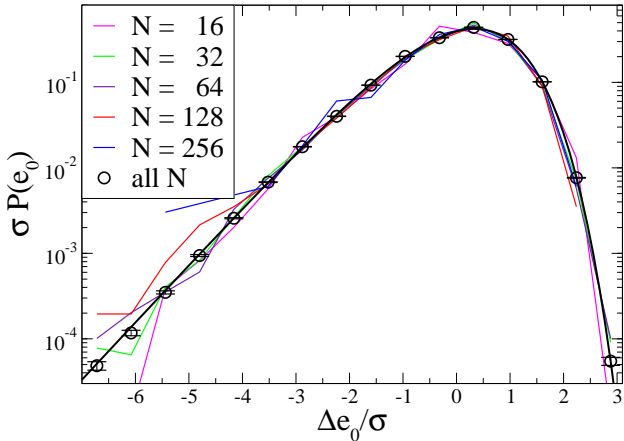


Figure 2. Distribution of ground state energy density fluctuations,  $P(e_0)$ , as a function of  $\Delta e_0 = e_0 - \langle e_0 \rangle$ , normalized by its deviation,  $\sigma = \sqrt{\langle \Delta e_0^2 \rangle}$ . Note that finite size effects are imperceptibly small, as indicated by the colored thin lines for a range of system sizes  $N$ . Thus, data for all sizes  $N \geq 16$  have been combined ( $\circ$ ) and fitted with a Gumbel distribution with a parameter of  $m \approx 0.87$  (thick solid line).

form

$$C_N \sim \frac{\ln N}{N}, \quad (4)$$

as is found exactly in REM. Indeed, when we again fix  $\langle e_0 \rangle_{\infty}^{p=3}$  and now fit the data in Tab. I according to the FSC in Eq. (3) asymptotically for large enough  $N$ , we do obtain a stable fit, as is shown in Fig. 1. There, we have even allowed for a  $C_N^2$  correction (dashed line) that closely fits the data for all  $N \geq 32$ .

We have probed the 3-spin model also for another of the subtle properties that FSC in the ground state energies in SK exhibit. In Ref. [18], it was found that in a bond-diluted version of SK, where  $q$  is the fraction of non-zero bonds, the FSC exhibit a power-law dependence with an exponent  $\omega = \omega(q)$  that varies with  $q$ , as shown in the inset of Fig. 1. Already cursory exploration of the 3-spin model at  $q = 0.25$  alone, with the data listed in Tab. I and also plotted in Fig. 1, strongly suggests that there is no such variation with  $q$  here. Unlike for SK, this data (appropriately rescaled by  $1/\sqrt{q}$  [26]) neatly collapses onto that of the undiluted version ( $q = 1$ ) for all but the smallest sizes  $N$ , showing that its FSC are likely identical at leading order, as in Eq. (4). Since this form of  $C_N$  does not have an anomalous exponent that would allow a variation with  $q$  to begin with, the observed lack of variation further speaks in favor of such a form.

Considering the distribution of ground state energies over the ensemble,  $P(e_0)$ , we find that it is rather close to a simple Gumbel distribution expected for an extreme value statistic for the lowest in a spectrum of *iid* random energies, as can be calculated exactly for REM. As shown in Fig. 2, there its very little variation in the

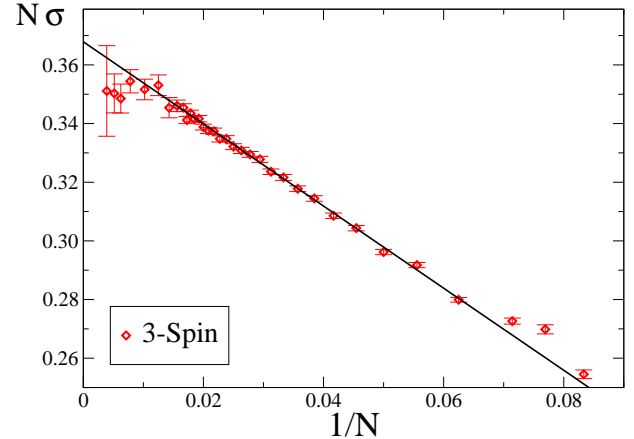


Figure 3. Extrapolation plot for the finite size corrections of the deviation  $\sigma$  of the distribution of ground state energies in Fig. 2. The data suggests that  $\sigma$  is simply a series in  $1/N$ , although logarithmic corrections can not be entirely excluded.

shape of that distribution, appropriately normalized via its standard deviation, for the data shown. Thus, we have combined all data for  $16 \leq N \leq 256$  listed in Tab. I to improve statistics especially in the exponentially small tails of  $P(e_0)$ , resulting in a very stable set of data points. Fitting those with a generalized Gumbel distribution in the form of

$$\ln P(e_0) = A + m [(x - u)/v - \exp\{(x - u)/v\}], \quad (5)$$

using the rescaled variable  $x = (e_0 - \langle e_0 \rangle)/\sigma$  with deviations  $\sigma(e_0) = \sqrt{\langle e_0^2 \rangle - \langle e_0 \rangle^2}$ , yields  $m = 0.87(5)$ ,  $A = 0.50(4)$ ,  $u = 0.33(5)$ , and  $v = 1.27(4)$ . Note the proximity of  $m$  to unity, marking a pure Gumbel distribution, as found in REM. A corresponding fit to the ground state data in SK is far less skewed, with a parameter of  $m \approx 5$  [21], far more distinct from REM. The deviation itself appears to vary with a simple  $1/N$  corrections, as demonstrated in Fig. 3, potentially with logarithmic factors that are hard to discern at this scale. This behavior of the 3-spin model, again, matches more closely with REM (which has  $\sigma \sim \ln N/N$ ) than SK, for which it was derived [27] that  $\sigma \sim N^{-\frac{5}{6}}$ , a rare exact finite size result for SK.

Finally, we have also measured the distribution  $P(h)$  of local fields  $h_i$  that are impinging on each spin  $\sigma_i$  due to the coupling it has to all its neighbors in the ground state,

$$h_i = \sum_{j < h; i \neq j, k} J_{ijk} \sigma_j \sigma_k. \quad (6)$$

This distribution is shown for select values of  $N$  in Fig. 4. Its behavior is quite similar to that observed for SK at finite  $N$  [28]. The distribution is somewhat broader here but similarly develops a pseudo-gap, i.e.,  $P(h) \rightarrow 0$

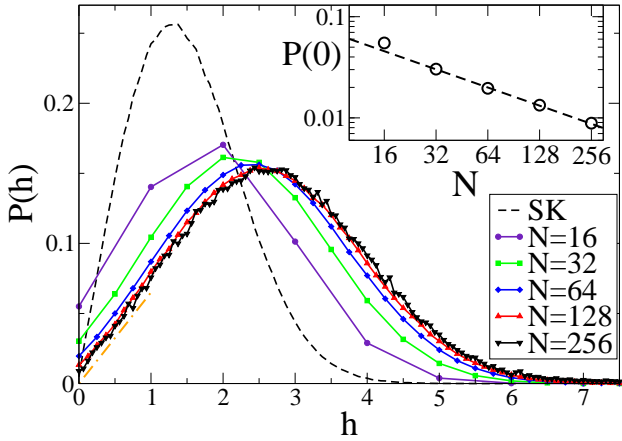


Figure 4. Plot of the distribution  $P(h)$  of local fields  $h$  impinging on spins by their neighbors in the ground state configurations of the 3-spin model, plotted for different system sizes. (Since  $P(h)$  is symmetric in  $h$ , only values for  $h \geq 0$  are shown.) Although significant finite-size effects are apparent, there is only a small variation between the two largest sizes, suggesting that the shape for  $P(h)$  at  $N = 256$  is close to the thermodynamic limit. For reference, the corresponding distribution for SK is provided (dashed line). The orange dash-dotted line refers to Eq. (7). The values for  $P(h = 0)$  appear to evolve to zero, such that the distribution has a pseudo gap in the thermodynamic limit. The inset suggests that  $P(0) \sim N^{-\alpha}$  for  $N \rightarrow \infty$  with  $\alpha \approx 0.6$  (dashed line).

linearly for  $h \rightarrow 0$ , in the thermodynamic limit. At finite size and near the origin, it appears that we can make a linear fit,

$$P(h) \sim AN^{-\alpha} + Bh, \quad (7)$$

with parameters  $\alpha \approx 0.6$ ,  $A \approx 0.24$ , and  $B \approx 0.06$  (see inset of Fig. 4).

To achieve our results for the  $p$ -spin model to this value in size,  $N = 256$ , we have implemented the extremal optimization heuristic (EO) [29, 30] similar to the version used for SK in Ref. [21] in a vectorized form[31] on a GPU. To this end, we have also compressed both, the binary spin variables as well as the discrete bimodal bond-distribution ( $J = \pm 1$  on one bit for the complete graph or  $J = 0, \pm 1$  on two bits for the dilute system), into a bit-wise form such that a single byte with 32-bits in the GPU can hold either 32 or 16 bonds. Although higher system sizes than  $N = 256$  could have been reached with this implementation, the necessary runtime to obtain stable results increased significantly faster than for similar studies of SK [21], as is shown in Fig. 5. This might be caused by the fact that local search in the 3-spin model exhibits the “overlap gap condition” which entails a far more complex energy landscape to explore than for SK [14]. Yet, using asymptotic extrapolations of our finite-size data clearly makes a connection with the true thermodynamic limit. Furthermore, the use of such an extrapolation plot (like

Fig. 1) of finite size data also proves to be a powerful

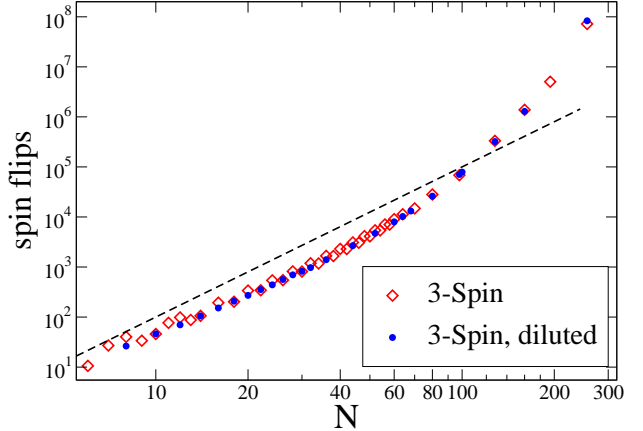


Figure 5. Plot of the average number of spin flips needed to reach the presumed ground state energy for each system size  $N$ , both for the complete system (red  $\diamond$ ) and systems diluted to 25% of bonds (blue  $\bullet$ ). The maximal runtime is initially set to be at least  $0.1N^3$  spin flips (dashed line) but adaptively increased such that always twice as many flips are used as were needed to find the latest new optimum. With that criterion, runtimes escalate rapidly for larger  $N$  and become prohibitive above  $N = 256$ .

technique to assess the scalability of a heuristic, beyond the use of static testbeds [6], since low- $N$  ensemble averages often yield sufficient bounds on the expected large- $N$  behavior to estimate systematic errors and detect their divergence [32, 33].

In conclusion, we have provided the first systematic study of the  $T = 0$  properties of the 3-spin model at finite size  $N \leq 256$  that can serve as a benchmark for future comparisons. The results of our extensive simulations for the ground state energies, an NP-hard problem tackled with a sophisticated heuristic here, prove to be sufficiently accurate at such large sizes that we can draw strong conclusions about the nature of finite-size corrections by which the model extrapolates to the thermodynamic limit. In the context of the generalized  $p$ -spin model, we highlight the stark contrast in this behavior between the case of  $p = 3$  here and the Sherrington-Kirkpatrick model ( $p = 2$ ) on one side, and on the other side the close resemblance with the REM ( $p = \infty$ ), indicating how special SK is while all models with  $p \geq 3$  appear to share the same finite size corrections to their ground state behavior with REM.

*Acknowledgements:* We like to thank Ahmed El-Alaoui and Andrea Montanari for inspiration and fruitful correspondences. SB thanks Federico Ricci-Tersenghi and Lenka Zdeborova for helpful insights on the  $p$ -spin model. Some of the computations were conducted on the Emory Hyper Community Cloud Cluster (<https://it.emory.edu/catalog/cloud-services/hyperc3.html>).

---

[1] S. F. Edwards and P. W. Anderson, *J. Phys. F* **5**, 965 (1975).

[2] D. Sherrington and S. Kirkpatrick, *Phys. Rev. Lett.* **35**, 1792 (1975).

[3] P. Charbonneau, E. Marinari, and M. Mezard, eds., *Spin glass theory and far beyond* (World Scientific, Singapore, 2023).

[4] M. Mézard and A. Montanari, *Constraint Satisfaction Networks in Physics and Computation* (Oxford University Press, Oxford, 2006).

[5] G. Kochenberger, J.-K. Hao, F. Glover, M. Lewis, Z. Lü, H. Wang, and Y. Wang, *Journal of Combinatorial Optimization* **28**, 58 (2014).

[6] S. Boettcher, *Physical Review Research* **1**, 033142 (2019).

[7] C. C. McGeoch and C. Wang, in *Proceedings of the ACM International Conference on Computing Frontiers*, CF '13 (ACM, New York, NY, USA, 2013) pp. 23:1–23:11.

[8] T. Albash, T. Ronnow, M. Troyer, and D. Lidar, *The European Physical Journal Special Topics* **224**, 111 (2015).

[9] G. Rosenberg, M. Vazifeh, B. Woods, and E. Haber, *Computational Optimization and Applications* **65**, 845 (2016).

[10] H. Goto, K. Tatsumura, and A. R. Dixon, *Science Advances* **5**, eaav2372 (2019).

[11] H. Goto, K. Endo, M. Suzuki, Y. Sakai, T. Kanao, Y. Hamakawa, R. Hidaka, M. Yamasaki, and K. Tatsumura, *Science Advances* **7**, eabe7953 (2021).

[12] M. Aramon, G. Rosenberg, E. Valiante, T. Miyazawa, H. Tamura, and H. G. Katzgraber, *Frontiers in Physics* **7**, 10.3389/fphy.2019.00048 (2019).

[13] D. Gamarnik, *Proceedings of the National Academy of Sciences* **118**, 10.1073/pnas.2108492118 (2021).

[14] A. E. Alaoui and A. Montanari, *arxiv:2009.11481* (2020).

[15] B. Derrida, *Phys. Rev. Lett.* **45**, 79 (1980).

[16] B. Derrida, *Phys. Rev. B* **24**, 2613 (1981).

[17] M. R. Garey and D. S. Johnson, *Computers and Intractability: A Guide to the Theory of NP-Completeness* (W. H. Freeman, New York, 1979).

[18] S. Boettcher, *Physical Review Letters* **124**, 177202 (2020).

[19] W. Wang, *Physical Review B* **106**, 134209 (2022).

[20] E. Gardner, *Nuclear Physics B* **257**, 747 (1985).

[21] S. Boettcher, *The European Physical Journal B* **46**, 501 (2005).

[22] T. Aspelmeier, A. Billoire, E. Marinari, and M. A. Moore, *Journal of Physics A: Mathematical and Theoretical* **41**, 324008 (2008).

[23] S. Boettcher, *Journal of Statistical Mechanics: Theory and Experiment* **2010**, P07002 (2010).

[24] A. Montanari and F. Ricci-Tersenghi, *The European Physical Journal B - Condensed Matter* **33**, 339 (2003).

[25] J. Yeo and M. A. Moore, *Physical Review E* **101**, 032127 (2020).

[26] P. Carmona and Y. Hu, *Annales de l'Institut Henri Poincaré (B) Probability and Statistics* **42**, 215 (2006).

[27] G. Parisi and T. Rizzo, *Phys. Rev. Lett.* **101**, 117205 (2008).

[28] S. Boettcher, H. G. Katzgraber, and D. Sherrington, *Journal of Physics A: Mathematical and Theoretical* **41**, 324007 (2008).

[29] S. Boettcher and A. G. Percus, *Physical Review Letters* **86**, 5211 (2001).

[30] S. Boettcher and A. Percus, *Artificial Intelligence* **119**, 275 (2000).

[31] The details of this implementation will be discussed elsewhere.

[32] S. Boettcher, *Nature Machine Intelligence* **5**, 24 (2022).

[33] S. Boettcher, *Nature Communications* **14**, 5658 (2023).